(Preprint) AAS 09-443

LOW-ENERGY BALLISTIC TRANSFERS TO LUNAR HALO ORBITS

Jeffrey S. Parker*

Recent lunar missions have begun to take advantage of the benefits of low-energy ballistic transfers between the Earth and the Moon rather than implementing conventional Hohmann-like lunar transfers. Both Artemis and GRAIL plan to implement low-energy lunar transfers in the next few years. This paper explores the characteristics and potential applications of many different families of low-energy ballistic lunar transfers. The transfers presented here begin from a wide variety of different orbits at the Earth and follow several different distinct pathways to the Moon. This paper characterizes these pathways to identify desirable low-energy lunar transfers for future lunar missions.

INTRODUCTION

The Exploration Program's call to return humans to the Moon requires a means to transfer large quantities of cargo to and from the Moon for low cost. The cargo may be lunar habitats, vehicles, fuel, supplies, and even support satellites for the explorers. In later phases, the cargo may be raw materials mined from the Moon to be shipped back to the Earth. One way to reduce the transport cost is to use low-energy transfers, i.e., non-Keplerian trajectories that require less fuel than conventional transfers. The Artemis and GRAIL mission designs have demonstrated the benefits of these low-energy lunar transfers.[1,2] It is now of interest to characterize all the different types of low-energy ballistic transfers that exist between the Earth and the Moon and their applications to practical lunar missions.

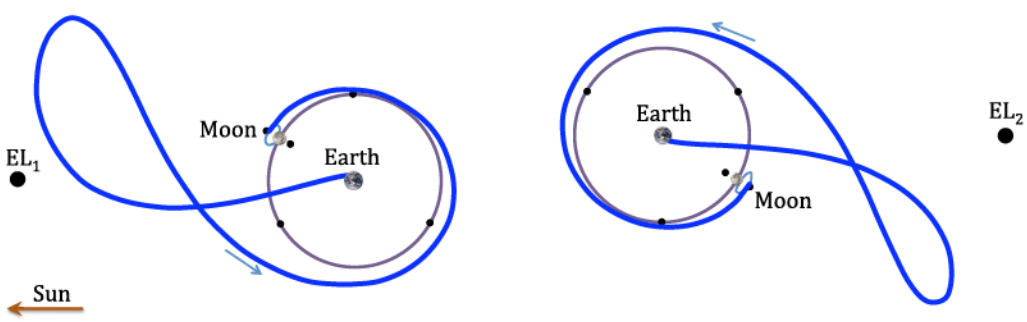

Figure 1 Two example low-energy ballistic transfers between the Earth and a halo orbit on the far side of the Moon, viewed from above in the Sun-Earth synodic reference frame. Planetary images courtesy of NASA

Low-energy ballistic lunar transfers (BLTs) are trajectories that a spacecraft may take to ballistically transfer between the Earth and Moon using less energy than a conventional, direct lunar transfer. Rather than traveling directly from the Earth to the Moon in just a few days, a spacecraft

*Staff Engineer, Jet Propulsion Laboratory, California Institute of Technology, 4800 Oak Grove Dr., Pasadena, CA 91109

on a low-energy BLT travels beyond the Moon and spends three or more months taking advantage of the Sun's gravity to raise its energy. The spacecraft arrives at the Moon in such a way that it may insert into a large three-body orbit, such as a halo or Lissajous orbit, for virtually no fuel; or it may insert into a low lunar orbit or land on the surface of the Moon using less fuel than if it had arrived from a conventional, direct transfer.[3] Figure 1 shows two example low-energy transfers between the Earth and a halo orbit on the far side of the Moon. The transfers are viewed from above in the Sun-Earth synodic reference frame.

This paper takes advantage of dynamical systems theory to generate low-energy transfers between the Earth and lunar halo orbits. Previous studies have demonstrated the benefits of using dynamical systems theory to construct, analyze, and categorize low-energy lunar transfers in simplified models of the solar system.[3–8] This paper studies the problem of generating low-energy transfers in the full ephemeris model of the solar system, taking into account accurate locations and orbits of each of the planets in the solar system. Many of the dynamical systems methods that have been shown to be successful in a simplified model of the solar system are just as successful in the ephemeris model. This paper presents the process of constructing low-energy transfers, categorizing those transfers into families, and analyzing those families, all in the ephemeris model of the solar system.

This paper first presents the background of dynamical systems theory and low-energy lunar transfers. It then presents the method used here to construct low-energy lunar transfers using dynamical system theory. This method provides an easy way to categorize lunar transfers into organized families. The paper studies these families and considers how they vary from month to month. Finally, the paper provides a discussion of practical applications of this research to lunar missions.

BACKGROUND

This section presents the models and dynamical systems tools that have been used in this research to construct and analyze BLTs.

Models

The trajectories produced in this paper are significantly influenced by the gravitational forces of two or more massive bodies. In order to understand the characteristics of these non-Keplerian trajectories, it is useful to explore simplified models of the solar system. The Circular Restricted Three-Body Problem (CRTBP) describes a convenient system to model the motion of a spacecraft in the presence of two massive bodies that orbit their barycenter in circular orbits. The model formulated by the CRTBP is a good first approximation for spacecraft trajectories in the solar system since many planets and natural satellites traverse orbits that are nearly circular. Low-energy lunar transfers, however, involve the gravitational interactions of the Sun, Earth, and Moon. The Patched Three-Body Model provides a simple model that includes all three massive bodies while retaining the beneficial components of the CRTBP. Finally, the Jet Propulsion Laboratory's DE421 Planetary and Lunar Ephemerides is used to produce trajectories that are close approximations to real trajectories in the solar system.

Circular Restricted Three-Body Problem (CRTBP)

The Circular Restricted Three-Body Problem[9] describes a dynamical model that is used to characterize the motion of a massless particle, e.g., a spacecraft, in the presence of two massive bodies,

e.g., the Earth and the Moon. The model assumes the two massive bodies orbit their barycenter in circular orbits.

It is convenient to characterize the motion of the third body, i.e., the spacecraft, in a reference frame that rotates at the same rate as the orbital motion of the two primary masses. The coordinate frame is centered at the barycenter of the system and oriented such that the x-axis extends from the barycenter toward the smaller primary, the z-axis extends toward the primary bodies' orbit normal, and the y-axis completes the right-handed coordinate frame. In that synodic frame, the two massive bodies are stationary and the spacecraft moves about the system in non-Keplerian motion.[3,9] It is convenient to normalize the units in the system such that the following measurements are equal to one: the distance between the two primaries, the sum of the mass of the two primaries, the rotation rate of the system, and the gravitational parameter. The equations of motion for the third body in the normalized rotating frame are equal to:[9]

$$\ddot{x} = 2\dot{y} + x - (1-\mu)\frac{x+\mu}{r_1^3} - \mu\frac{x-1+\mu}{r_2^3} \tag{1}$$

$$\ddot{y} = -2\dot{x} + y - (1-\mu)\frac{y}{r_1^3} - \mu\frac{y}{r_2^3} \tag{2}$$

$$\ddot{z} = -(1-\mu)\frac{z}{r_1^3} - \mu\frac{z}{r_2^3} \tag{3}$$

where r_1 and r_2 are equal to the distance from the third body to the larger and smaller primary, respectively:

$$r_1^2 = (x+\mu)^2 + y^2 + z^2 \tag{4}$$

$$r_2^2 = (x-1+\mu)^2 + y^2 + z^2 \tag{5}$$

The spacecraft's position and velocity coordinates in Equations 1 – 5 are given in nondimensional normalized synodic coordinates; the parameter μ is the three-body constant, computed for the Earth-Moon system by dividing the Moon's mass by the total mass in the system. In this form it is clear that the dynamics of the system depend only on the mass fraction μ. Furthermore, as μ goes to zero, the dynamics approach two-body dynamics, although represented in a rotating frame.

There are five well-known equilibrium solutions to the CRTBP, known as the five Lagrange, or libration, points.[9] These points are referred to as L_1 – L_5; this paper adopts the nomenclature that L_1 lies between the two primary masses and L_2 lies on the far side of the smaller primary, relative to the barycenter of the system. The Lagrange points in the Earth-Moon system are abbreviated using the nomenclature LL_1 – LL_5; the Sun-Earth/Moon Lagrange points are abbreviated EL_1 – EL_5. The seven Lagrange points near the Earth are depicted in Figure 2.

Patched Three-Body Model

The Patched Three-Body Model[3,6–8] uses purely three-body dynamics to model the motion of a spacecraft in the presence of the Sun, Earth, and Moon. It retains many of the desirable characteristics of the CRTBP, while permitting a spacecraft in the near-Earth environment to be affected by all three massive bodies, albeit only two massive bodies at any given moment. When the spacecraft is near the Moon, the spacecraft's motion is modeled by the Earth-Moon three-body system. Otherwise, the spacecraft's motion is modeled by the Sun-Earth three-body system, where the secondary body is the barycenter of the Earth and Moon. For simplicity it is assumed that the Earth-Moon system is coplanar with the Sun-Earth system. The boundary of these two systems is referred to as the

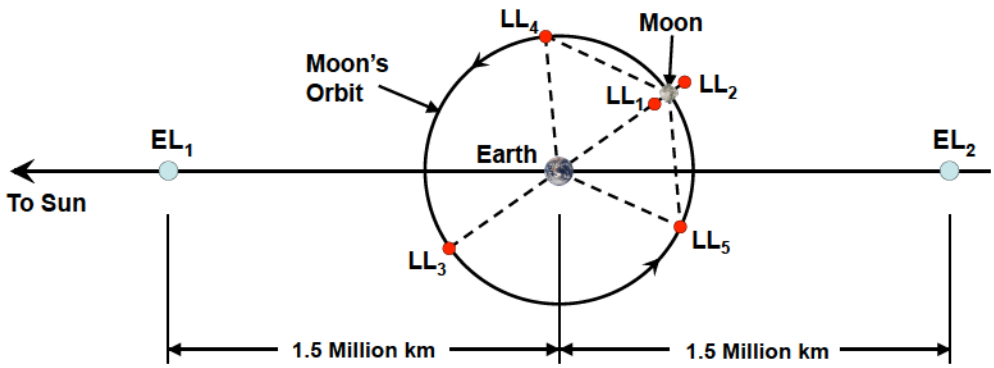

Figure 2 A plot depicting the relative proximity of the five Earth-Moon Lagrange points and the two nearby Sun-Earth Lagrange points. Planetary images courtesy of NASA.

three-body sphere of influence (3BSOI); it is analogous to the two-body sphere of influence used in the patched conic method of interplanetary mission design. The 3BSOI is described as the boundary of a sphere centered at the Moon with a radius r_{SOI} computed using the following relationship:

$$r_{\text{SOI}} = a \left(\frac{m_{\text{Moon}}}{m_{\text{Sun}}} \right)^{2/5} \tag{6}$$

where m_{Moon} and m_{Sun} are the masses of the Moon and Sun, respectively, and a is the average distance between the Sun and Moon, equal to approximately 1 AU. Thus, the three-body sphere of influence has a radius of approximately 159, 200 km. A sphere of that radius centered at the Moon includes the Moon's L_1 and L_2 points, but not the other three Lagrange points.

JPL DE421 Planetary and Lunar Ephemerides

The Jet Propulsion Laboratory and the California Institute of Technology has developed the DE421 Planetary and Lunar Ephemerides, which is the most accurate model of the solar system used in this research. The model includes ephemerides of the positions and velocities of the Sun, the four terrestrial planets, the four gas-giant planets, the Pluto/Charon system, and the Moon.[10] The lunar orbit is accurate to within a meter and the orbits of Earth, Mars, and Venus are accurate to within a kilometer.[10]

Halo Orbits in the CRTBP

The CRTBP permits the existence of many classes of orbits, including periodic and quasiperiodic two- and three-dimensional orbits.[3] Halo orbits are very interesting and well-known periodic three-dimensional solutions to the CRTBP.[11–14]

Many authors have studied how to take advantage of lunar halo orbits for practical missions to the Moon.[12,15,16] Halo orbits are of particular use for lunar communication and navigation satellites.[17,18] Figure 3 shows plots of example halo orbits about LL_1 and LL_2. Since the force field in the CRTBP is symmetric about the $x - y$ plane, and since halo orbits are asymetric about this plane, each halo orbit solution to the CRTBP comes in a symmetric pair. The two varieties of halo orbits are known as Northern and Southern orbits.[13] As one can see in Figure 3, a satellite in a Southern

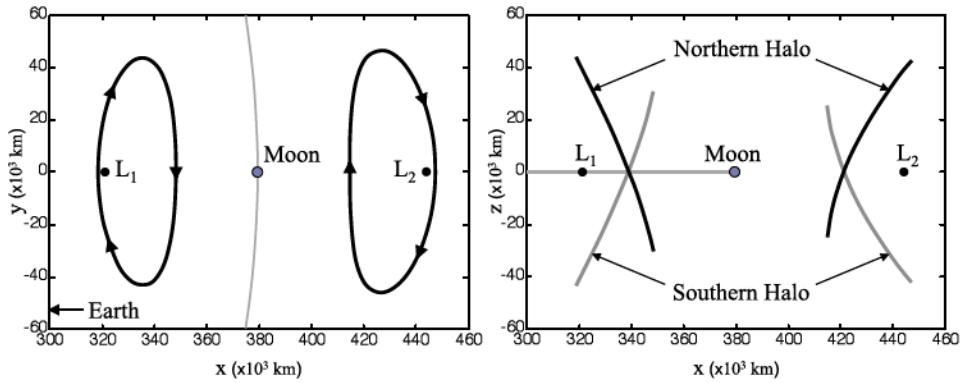

Figure 3 Two perspectives of example halo orbits about the lunar L_1 and L_2 points. Left: the halo orbits viewed from above in the Earth-Moon synodic reference frame; Right: the halo orbits viewed from the side.

orbit spends more than half of its time below the $x - y$ plane, which gives that satellite benefits for communicating with objects in the Southern hemisphere of the Moon.

Halo orbits do not have a constant set of orbital elements like conic orbits. However, halo orbits exist in well-defined families, a characteristic that allows a particular halo orbit in a family to be uniquely specified by a single parameter.[19] It is convenient to specify a halo orbit by its z-axis amplitude, A_z, since one may formulate an analytical approximation to a halo orbit using that parameter as an input.[20–22] Other studies have specified a halo orbit using its Jacobi constant or its x_0-value, namely, the x-value of the location where the halo orbit pierces the x-axis with positive y-velocity.[3,14] Figure 4 shows several Northern LL_1 and LL_2 halo orbits from the side in the synodic reference frame to illustrate the relationship between a halo orbit's shape and its z-axis amplitude. Figure 5 shows the relationship between a halo orbit's z-axis amplitude and its period for reference.

In this research, a halo orbit in the CRTBP is specified within its family by A_z. A second parameter, F, may be used to specify which family of halo orbits is being considered, e.g., *Southern LL_2*

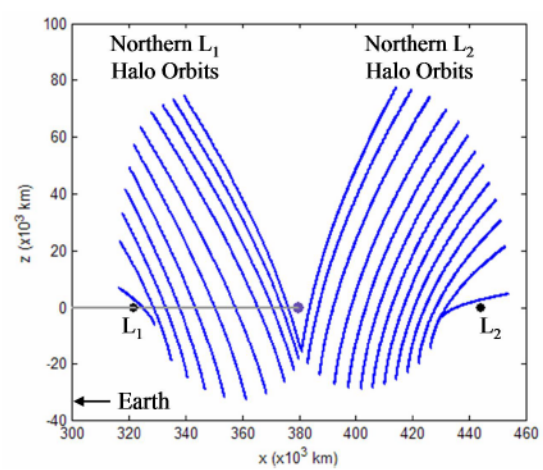

Figure 4. Northern Earth-Moon Halo Orbits

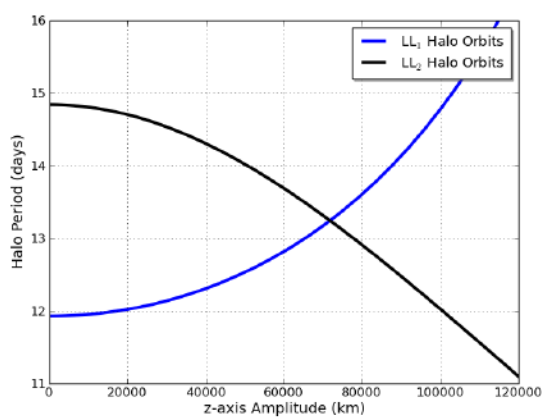

Figure 5. Halo Orbit Periods

halo orbits. Once a halo orbit is specified, a third parameter, τ, may be used to identify a single point in that orbit. This study defines τ analogous to a conic orbit's true anomaly, sweeping out 360° per revolution of the halo orbit, such that τ is equal to 0° at the orbit's first x-axis crossing that has positive y-axis velocity.

Halo Orbits in the Solar System

Halo orbits are only truly periodic in simplified models of the solar system, such as the CRTBP. Since the real solar system includes numerous perturbations, particularly the non-zero eccentricity of the Sun, Earth, and Moon about their respective barycenters, a spacecraft traversing a halo orbit does not retrace its path perfectly from one revolution to the next. The quasi-halo trajectories generated in this research have been constructed by first approximating them using the Richardson analytical expansion[21] and then differentially correcting that approximation into the DE421 ephemeris model of the solar system using a multiple shooting differential corrector. The multiple shooting differential corrector takes a series of trajectory states and adjusts them in order to make the entire trajectory continuous.[14,22,23] The differential correction process is described in more detail in Appendix A.

Figure 6 shows the difference between a halo orbit about LL_2 produced in the CRTBP compared with the same halo orbit differentially-corrected into the DE421 model of the solar system. One can see that the DE421 halo orbit is quasiperiodic, tracing out the same vicinity of space on each orbit, but never truly retracing itself.

It is interesting to observe that many halo orbits in the DE421 model of the solar system come much closer to repeating their paths every other revolution. This is due to the fact that many halo orbits have a revolution period that is approximately half of the orbital period of the two primary bodies in the three-body system. Since the Moon is orbiting the Earth-Moon barycenter in an elliptical orbit, the geometrical characteristics of a halo orbit depend on where the Moon is along its orbit. Every other halo orbit will follow the Moon in approximately the same portion of its orbit.

The differential correction process typically causes the endpoints of a trajectory to shift much more dramatically than the interior states along the trajectory, assuming that the endpoints are not

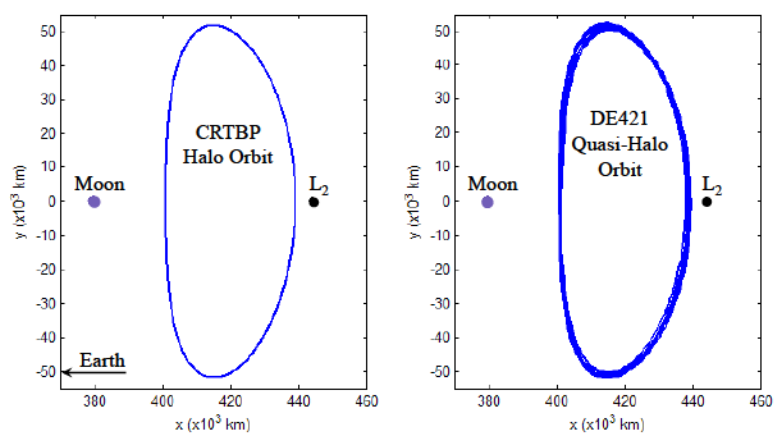

Figure 6 A comparison between a halo orbit produced in the CRTBP and a quasi-halo orbit produced in the DE421 model of the solar system. The orbits are shown in the Earth-Moon synodic reference frame.

constrained in any additional way. This research implements a method that involves differentially correcting many revolutions of an approximate halo orbit together and then pruning the resulting trajectory in order to generate a trajectory that remains very near the desired reference halo orbit. This two-step process is illustrated in Figure 7. The DE421 halo orbits generated in this paper have been constructed by differentially correcting four revolutions of a halo orbit and then discarding the first and last revolutions, keeping the two interior revolutions.

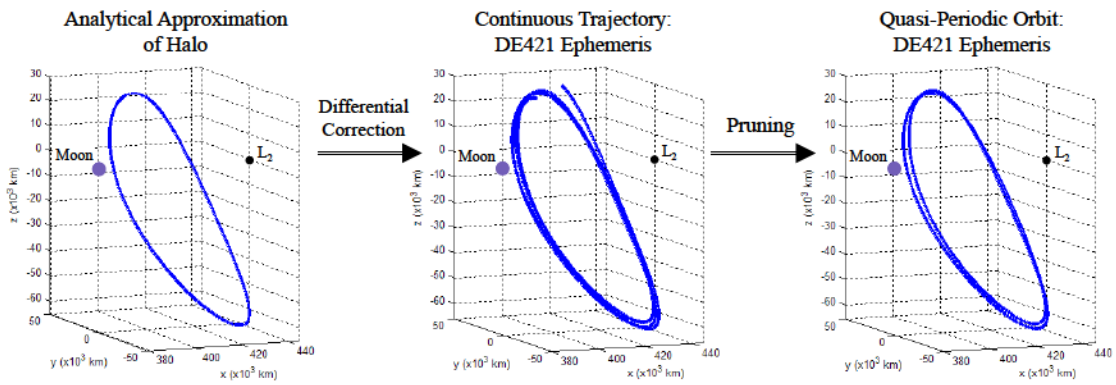

Figure 7 An example of the process of differentially-correcting and pruning a halo orbit from the Earth-Moon CRTBP into the DE421 Ephemeris model. Left: the nominal periodic halo orbit in the Earth-Moon CRTBP; Center: the differentially-corrected trajectory in the DE421 Ephemeris model; Right: the pruned quasiperiodic halo trajectory in the DE421 Ephemeris model.

Each state along a halo trajectory generated in the DE421 model of the solar system is designated by a τ-value, similar to a halo orbit generated in the CRTBP. However, each revolution of a halo trajectory in the DE421 model requires a slightly different duration of time to traverse due to the model's dynamical perturbations. This paper retains the definition of τ in the DE421 model by specifying that τ is always equal to $0°$ at each x-axis crossing with positive y-velocity. Therefore, the rate of change of τ varies slightly from orbit to orbit; but the reference $\tau = 0°$ definition is constant.

The final consideration in this discussion is that halo orbit trajectories generated in the DE421 ephemeris vary based on a reference date. In this study, the analytical approximation of the halo orbit is sent to the differential corrector with the specification that the orbit's first $\tau = 0°$ state is set to a reference epoch. The differential corrector will adjust that orbit slightly, but the reference epoch will typically be near $\tau = 0°$ for the converged trajectory.

In summary, a halo orbit in the DE421 model of the solar system may be specified by the z-axis amplitude used to model it, A_z, and by a reference epoch, T_{ref}, used to anchor it in the solar system. The reference epoch specifies the approximate date that the desired halo orbit pierces the x-axis with positive y-velocity. This research then inputs a total of four revolutions of an analytical estimate of the halo orbit into the multiple shooting differential corrector: two revolutions after the reference epoch plus one "buffer" revolution on each end. After the differential corrector converges on a continuous trajectory in the DE421 model of the solar system, the trajectory is pruned to only include two revolutions of the halo orbit. Then any point along the halo orbit may be specified using the parameter τ.

Invariant Manifolds

Trajectories in a model with two or more massive bodies may be either unstable or neutrally stable.[24] Theoretically, a particle with a perfectly specified state will remain on an unstable orbit indefinitely. In reality, the state of a spacecraft following an unstable orbit in the presence of any random perturbation will exponentially diverge over time from its nominal state along the orbit. The more unstable the orbit, the faster the spacecraft's deviation will grow. The station-keeping costs for spacecraft on unstable trajectories have historically been very low: on the order of 1 m/s per month or less for spacecraft in Sun-Earth/Moon three-body trajectories.[25–28] Although the unstable nature of a lunar halo trajectory adds station-keeping requirements to a lunar mission, that unstable nature also enables the capability to transfer to/from the orbit for very little fuel.

An orbit's *unstable invariant manifold* (W^U) contains the set of all trajectories that a particle will take if it is perturbed anywhere on that orbit in the direction of the local unstable eigenvector.[29,30] Similarly, an orbit's *stable invariant manifold* (W^S) contains the set of all trajectories that a particle may take to asymptotically arrive onto that orbit along the local stable eigenvector. Put another way, the orbit's stable invariant manifold is the set of all trajectories that a particle will take backward through time if it is perturbed in the direction of the local stable eigenvector. The invariant manifolds of libration orbits in the CRTBP have *interior* and *exterior* halves, where, for instance, the trajectories in the interior half of a lunar halo orbit's manifold immediately approach nearer to the Moon and vice versa. Figure 8 shows plots of the stable and unstable invariant manifolds of an example libration orbit about the Earth-Moon L_2 point. The interior manifold in each case propagates toward the Moon; the exterior manifold traverses away from the Earth and Moon.

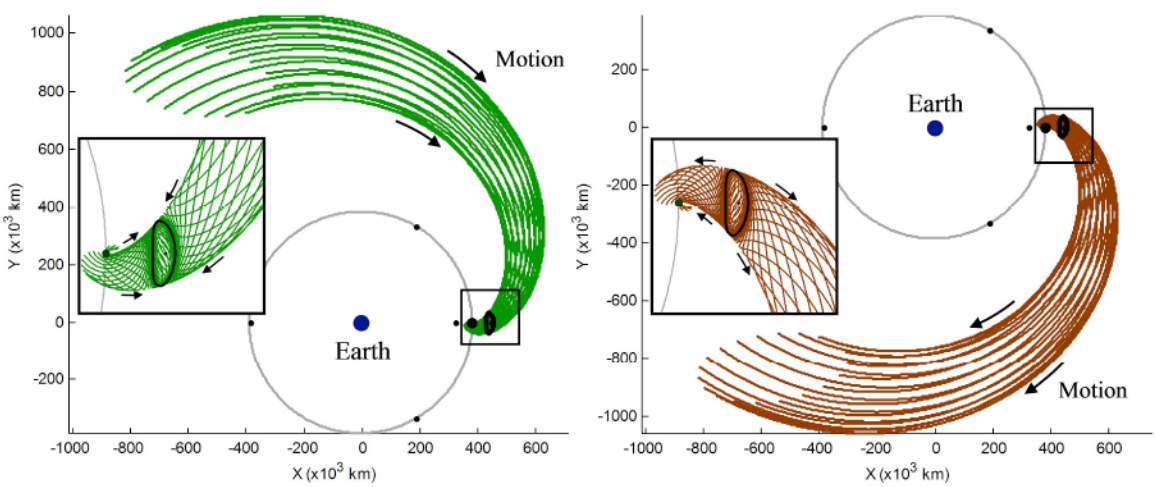

Figure 8 The stable (left) and unstable (right) manifolds of a libration orbit about the Earth-Moon L_2 point, viewed from above in the Earth-Moon synodic reference frame.

In practice, mission designers model an orbit's stable and unstable invariant manifolds by taking states along the orbit, perturbing them in an appropriate way, and integrating the resulting set of states through time.[3,31,32] The initial conditions $\mathbf{X}_0^S$ and $\mathbf{X}_0^U$ for the trajectories that may be used to model an orbit's stable and unstable manifolds, respectively, may be constructed using the following

equations:

$$\mathbf{X}_0^S = \mathbf{X}_0 \pm \epsilon \frac{\mathbf{v}^S}{|\mathbf{v}^S|} \tag{7}$$

$$\mathbf{X}_0^U = \mathbf{X}_0 \pm \epsilon \frac{\mathbf{v}^U}{|\mathbf{v}^U|}, \tag{8}$$

where $\mathbf{v}^S$ and $\mathbf{v}^U$ are the stable and unstable eigenvectors of the orbit's local state transition matrix, respectively, ϵ is the magnitude of the perturbation, and the sign of the perturbation differentiates between the interior and exterior halves of the orbit's manifolds. It is common to normalize the perturbations across the entire manifold such that the perturbations have a constant position magnitude, e.g., 100 km.[33]

As ϵ in Equations 7 and 8 is reduced to zero, the resulting trajectories more precisely model the orbit's manifold, however, it takes more propagation time for the trajectories to depart the host orbit. In the Earth-Moon three-body system, there is little practical difference between the set of trajectories that implements a perturbation of 10 meters and the set of trajectories that implements a perturbation of 10 km, assuming that the host orbit does not approach very close to either of the primary bodies. In practice, such small differences are overwhelmed by unmodeled variations in solar radiation pressure and other dynamical perturbations. This study assumes that in practice a spacecraft approaching an Earth-Moon three-body orbit along its stable manifold has arrived on the orbit once its state is within 100 km of the orbit; ϵ is therefore set to provide a normalized perturbation with a position magnitude of 100 km.

Low-Energy Ballistic Lunar Transfers

Many techniques have been used to transfer material between the Earth and the Moon. The conventional approach involves sending a spacecraft on a direct transfer, including a large maneuver at the Earth, a large orbit insertion maneuver at the Moon, and fewer than six days of transfer duration.[3,17] This approach has been used by many missions to send spacecraft to low lunar orbits, including the Apollo missions and the recent Lunar Reconnaissance Orbiter. By extending the transfer's duration by several months and taking advantage of the Sun's gravity to boost the spacecraft's energy relative to the Earth, one may substantially reduce or even eliminate the need for the second large maneuver. The two GRAIL spacecraft require smaller orbit insertion maneuvers to enter their low lunar orbits than they would if they implemented conventional direct transfers;[2] the two Artemis spacecraft require no deterministic orbit insertion maneuvers to enter their respective lunar libration orbits.[1] In every practical case studied, the longer lunar transfers require less energy than conventional transfers; hence, they are known as low-energy ballistic lunar transfers. Table 1 summarizes the high-level energy requirements of typical direct lunar transfers compared with those of typical low-energy lunar transfers. The transfers compared are representative, do not include any specific mission constraints or targets, and are meant to be used only for illustration purposes.

Low-energy lunar transfers have been explored in the past using several different strategies. As early as 1968, Charles Conley began using dynamical systems methods to construct such transfers, although the transfers he constructed were restricted to two dimensions. Conley's method involved constructing a trajectory that transferred from the Earth's vicinity to the Moon's vicinity through the neck region about one of the collinear libration points in the Earth-Moon system.[34]

In the late 1980s and early 1990s, Edward Belbruno began developing a method to construct lunar transfers using his Weak Stability Boundary (WSB) theory.[35–37] The method involves targeting the

Table 1 A comparison of the characteristics of different types of lunar transfers to 100 km low lunar orbits and to lunar halo orbits.[3,17] These values are representative values and should only be used for top-level considerations.

Transfer Type	Destination	Lunar Flyby?	Injection C3	Orbit Insertion ΔV	Duration
Direct	100 km orbit	No	-2.06 km^2/s^2	813 m/s	4.5 days
Direct	Halo orbit	No	-2.26 km^2/s^2	550 m/s	5.0 days
Direct	Halo orbit	No	-2.26 km^2/s^2	475 m/s	10 – 30 days
Low-Energy	100 km orbit	No	-0.6 km^2/s^2	644.0 m/s	90^+ days
Low-Energy	100 km orbit	Yes	-2.0 km^2/s^2	644.0 m/s	90^+ days
Low-Energy	Halo orbit	No	-0.6 km^2/s^2	0.0 m/s	90^+ days
Low-Energy	Halo orbit	Yes	-2.0 km^2/s^2	0.0 m/s	90^+ days

region of space that is in gravitational balance between the Sun, Earth, and Moon, without involving any three-body periodic orbits. Ballistic capture occurs when the spacecraft's two-body energy becomes negative, as illustrated by Yamakawa.[38] Viacheslav Ivashkin developed a very similar targeting method in the early 2000s.[39–42]

In the mid 1990s, other methods were developed to construct a lunar transfer that take advantage of the chaos in the Earth-Moon three-body system.[43,44] Transfers have been produced using these methods that require less energy than conventional, direct transfers, but require between nine months and several years of transfer time.

In 2000, Koon et al. constructed a planar lunar transfer that was almost entirely ballistic using the techniques involved in Conley's method.[4,5] Similar to Conley, Koon et al. constructed a transfer by targeting a trajectory within the interior of the stable invariant manifold of a planar libration orbit about the Earth-Moon L_2 point. Once inside the interior of the stable manifold, the spacecraft ballistically arrives at some temporarily-captured orbit about the Moon.

Recent research has demonstrated how to use dynamical systems theory to construct low-energy ballistic lunar transfers in three-dimensions.[3,6–8] This research has shown that a low-energy ballistic transfer may be modeled as a series of heteroclinic transfers between unstable three-body orbits in the Sun-Earth system and the Earth-Moon system. Much of this work has been performed in the Patched Three-Body Model, a useful model for studying the theory behind these orbit transfers. The present work extends this research by studying the characteristics of low-energy transfers to lunar halo orbits in the DE421 model of the solar system.

Figure 9 illustrates how a low-energy ballistic transfer may be modeled as a series of orbit transfers in the Patched Three-Body Model. A spacecraft departs the Earth on a trajectory that shadows the stable invariant manifold of an unstable three-body orbit in the Sun-Earth/Moon three-body system. The spacecraft does not arrive on that orbit, however, before it ballistically diverts and then shadows the unstable manifold of that orbit. The trajectory is designed to arrive in the stable manifold of an unstable three-body orbit in the Earth-Moon three-body system, e.g., an LL_2 halo orbit.

Ballistic transfers between the Earth and unstable Earth-Moon three-body orbits are easily identified by propagating the stable manifold of the target lunar three-body orbit backward in time and intersecting it with the Earth. The trajectories must be propagated long enough to give them sufficient time to depart the Moon's vicinity, enter the Sun-Earth three-body system, and fall back to the

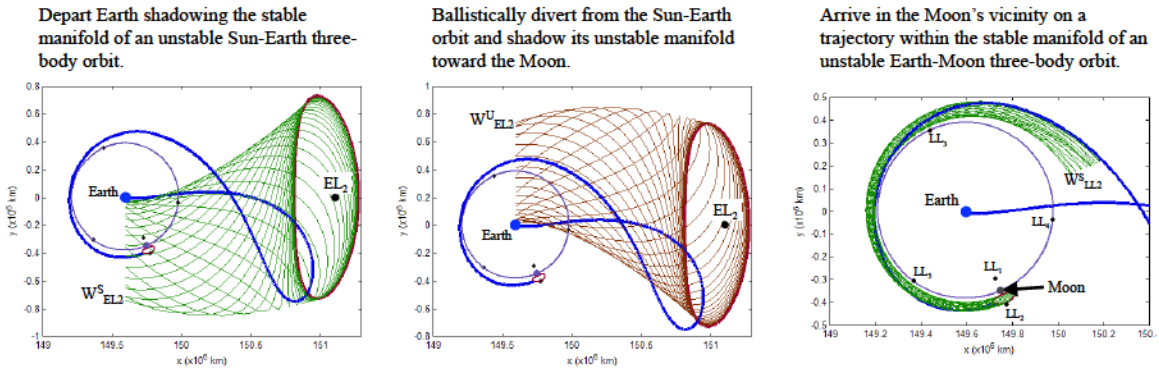

Figure 9 Modeling a ballistic lunar transfer as a series of heteroclinic transfers between unstable three-body orbits in the Patched Three-Body Model.

Earth. Some transfers require only 100 days to complete; others require more time due to additional revolutions about the Earth.

Dynamical systems theory provides the framework to parameterize a ballistic lunar transfer. A BLT in the Patched Three-Body Model may be characterized using six parameters:[3,7]

1. F: The family of unstable three-body orbits that includes the target lunar orbit, e.g., the family of Southern halo orbits about the LL_2 point.
2. A_z: The specific three-body orbit within the family F. Other papers interchange A_z with the orbit's Jacobi constant or x_0-value.
3. θ: The angle between the Sun-Earth axis and the Earth-Moon axis at the point of arrival at the lunar orbit.
4. p: The perturbation direction, i.e., whether the BLT implements the interior or exterior stable manifold of the lunar orbit.
5. τ: The arrival location on the lunar orbit, i.e., the specific trajectory within the orbit's stable manifold to traverse. This parameter is also directly related to the manifold's perturbation magnitude ϵ.
6. Δt_m: The propagation duration.

The first five parameters define the initial conditions for a trajectory that is then propagated backward in time for a duration of time equal to Δt_m. Assuming that the parameter set produces a BLT, the trajectory will have at least one close approach with the Earth when propagated backward in time. It may be the case that the first perigee passage does not encounter a desirable state to inject from, e.g., it may be at an undesirable altitude or inclination, but a later perigee passage does encounter a desirable injection state. The propagation duration Δt_m must be large enough to permit the trajectory to propagate to the best perigee passage.

BALLISTIC LUNAR TRANSFERS IN THE DE421 MODEL

The dynamical systems methods that enabled the clear analysis and construction of low-energy ballistic lunar transfers in the Patched Three-Body Model in previous studies apply to the DE421 model of the solar system as well. The Sun, Earth, and Moon orbit their respective barycenters in orbits that are not far from circular; the Moon's orbital plane is within 5.2 degrees of the Earth's orbital plane. Thus, many trajectories that exist in the Patched Three-Body Model are good approximations of trajectories that exist in the real solar system.

Low-energy ballistic lunar transfers are constructed in this study in the same way that they have been constructed in the Patched Three-Body Model. An unstable three-body orbit is selected as a target orbit near the Moon. The orbit's stable manifold is propagated and intersected with the Earth. Those trajectories that intersect the Earth may be used as ballistic transfers from the Earth to the target orbit via the orbit's stable manifold. The most significant adjustment to this procedure involves the construction of the target three-body orbit in the DE421 model. This process was described earlier in this paper. Ballistic lunar transfers may be uniquely specified in the DE421 model using a set of six parameters that is similar to the set used to describe transfers constructed in the Patched Three-Body Model. This set includes the parameters: $\{ F,\ A_z,\ T_{\text{ref}},\ p,\ \tau,\ \Delta t_m \}$, where T_{ref} specifies the reference epoch and replaces the parameter θ from the previous set of parameters.

Table 2 summarizes the set of parameters that generates an example BLT in the DE421 model, shown in Figure 10. The parameters F, A_z, and T_{ref} define the Southern LL_2 halo orbit that is shown in Figure 11. One can see that the multiple shooting differential corrector adjusted the state of the analytical approximation of the halo orbit such that the reference epoch is no longer at the $\tau = 0°$ point, but at the $\tau \approx 3.84°$ point. A particular trajectory in the halo orbit's stable manifold is then generated that corresponds to the parameters τ and p in Table 2, which propagates backward in time to a perigee with an altitude of 185 km. The distance between this trajectory and the Moon is shown in Figure 12. One can see that this trajectory asymptotically arrives at the orbit from the "Exterior" direction.

FAMILIES OF BALLISTIC LUNAR TRANSFERS

A set of BLT parameters may be used to generate the initial conditions of a trajectory that is propagated backward in time to construct a ballistic lunar transfer. If one set of parameters $\{ F',\ A'_z,\ T'_{\text{ref}},\ p',\ \tau',\ \Delta t'_m \}$ generates a trajectory that originates from a LEO orbit with an altitude of 185 km, then it is typically the case that a small deviation in either T'_{ref} or τ' will generate a trajectory that originates from a LEO orbit with a slightly different altitude. However, small deviations in both of those parameters may often be designed to generate a new trajectory that originates from a LEO orbit with the same 185 km altitude. In that case, the two sets of parameters define two different ballistic lunar transfers that are in the same family of transfers.

Figure 13 illustrates how BLTs may be organized into families. In this example, the BLT shown in Figure 10 with the parameters given in Table 2 is used as a reference trajectory. The BLT's parameters are all held constant, except for the parameters T_{ref} and τ, which are systematically varied through all combinations of values shown in Figure 13. At each combination, a new trajectory is propagated and analyzed to determine its new perigee altitude. One can see in Figure 13 that by reducing T_{ref} and increasing τ an appropriate amount, one can produce new trajectories that also have a perigee altitude of 185 km, and vice versa. By reducing both T_{ref} and τ, one builds trajectories

Table 2. The parameters used to produce the BLT shown in Figure 10.

Parameter	Value
F	The family of Southern Earth-Moon L_2 Halo Orbits
A_z	30,752 km (0.08 normalized distance units)
T_{ref}	15 January 2017 12:57:36 Ephemeris Time
τ	280.2°
p	"Exterior"
Δt_m	115.9 days

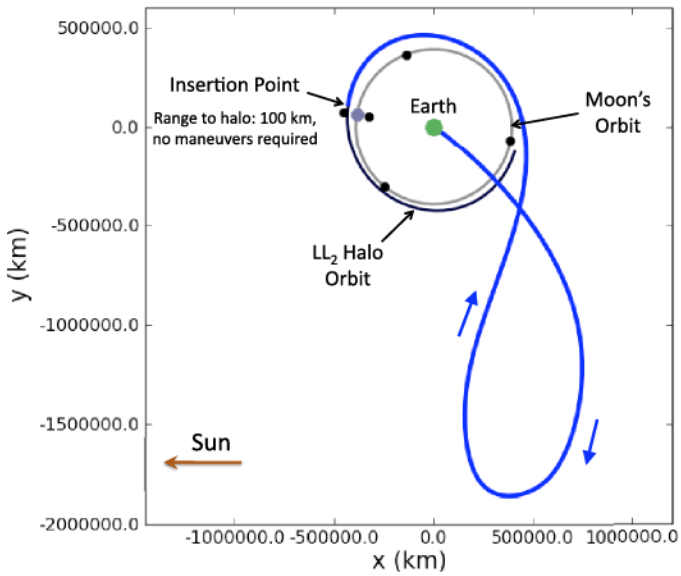

Figure 10. An example BLT produced in the DE421 model using the parameters specified in Table 2.

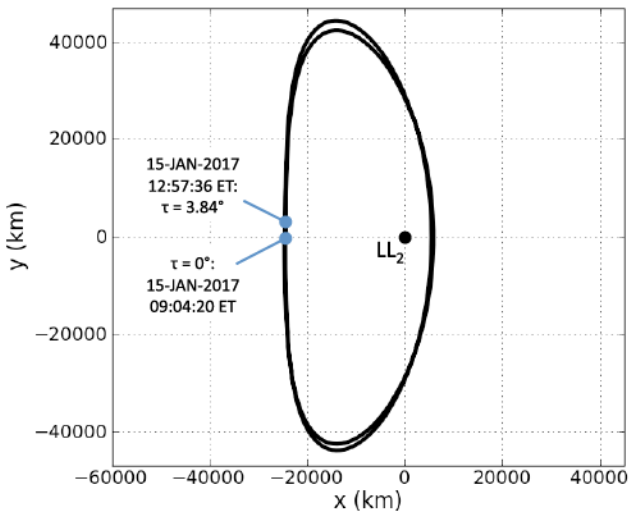

Figure 11. The halo orbit specified by F, A_z, and T_{ref} in Table 2.

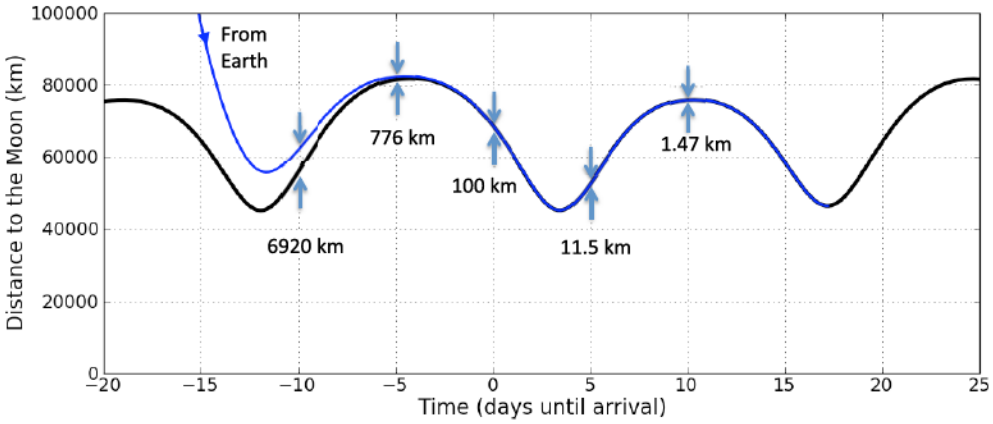

Figure 12 The distance between the BLT and the Moon as the trajectory approaches and arrives at the LL_2 halo orbit.

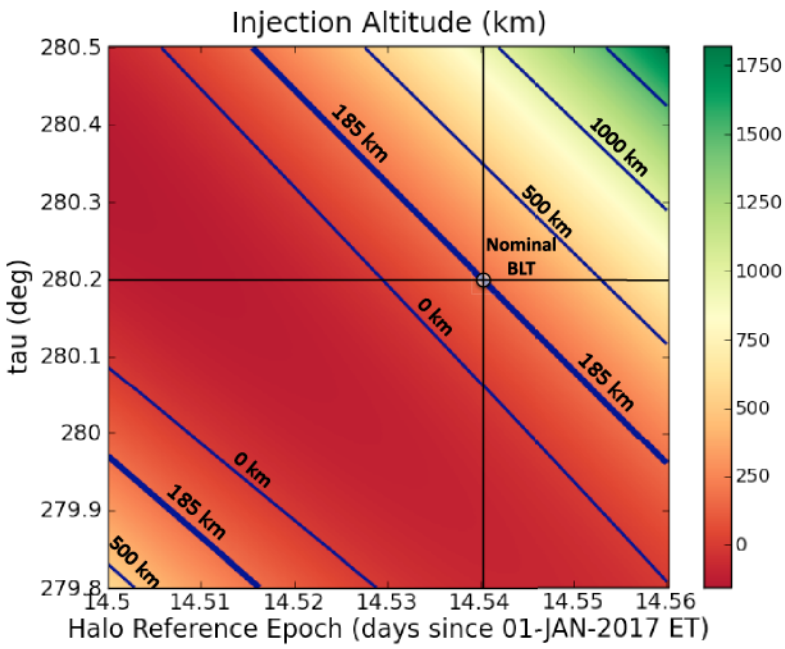

Figure 13 A map of the perigee altitude that each BLT trajectory encounters as a function of T_{ref} and τ. The 185-km contour is highlighted, which includes the nominal BLT presented in Table 2.

that come closer to the Earth at their perigee point, and vice versa.

The exercise given above may be extended to allow T_{ref} to vary across an entire month and τ to vary across 360° to observe full families of BLTs. Figure 14 shows such a state space map given the parameter set summarized in Table 3. The figure shows a plot that maps the perigee altitude of each trajectory generated using each combination of T_{ref} and τ. The darkest regions contain the parameters that produce useful BLTs; the white fields contain parameters that generate trajectories that never approach the Earth. Figure 15 shows the same map with several trajectories plotted to

Table 3. The parameters used to produce the results shown in Figure 14.

Parameter	Value
F	The family of Southern Earth-Moon L_2 Halo Orbits
A_z	30,752 km (0.08 normalized distance units)
T_{ref}	1 Jan 2017 00:00:00 ET $\leq T_{\text{ref}} \leq$ 31 Jan 2017 00:00:00 ET
τ	$0° \leq \tau \leq 360°$
p	"Exterior"
Δt_m	180 days

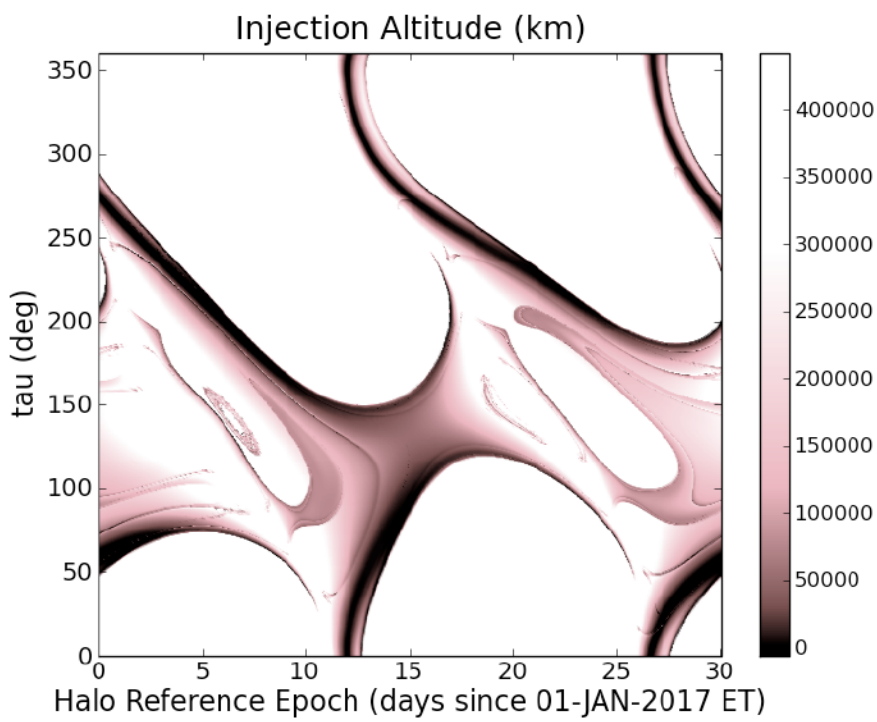

Figure 14 A state space map that shows the perigee altitude of each generated trajectory as a function of T_{ref} and τ. The darkest regions include the combinations of T_{ref} and τ that yield useful BLTs.

illustrate the trajectories that may be generated using these parameters.

Families of BLTs may be identified in the BLT state space map shown in Figure 14 by tracing those combinations of T_{ref} and τ that have a perigee altitude of some desirable value, e.g., 185 km. Figure 16 shows samples of the combinations of T_{ref} and τ that generate BLTs with injection altitudes of 185 km. The points displayed in black correspond to trajectories that traverse closer to EL_2 than EL_1 and vice versa. Table 4 presents a summary of the characteristics of a sample of the BLTs identified in Figure 16. Each of these BLTs is a member of a family of similar trajectories, whose characteristics vary smoothly away from those presented in the table. There are certainly many families of BLTs unrepresented in the table.

The quickest transfer identified in Figure 16 requires fewer than 83 days between the injection and the point when the trajectory has arrived within 100 km of the lunar halo orbit. The vast

Table 4 A summary of the characteristics of a sample of the BLTs identified in Figure 16. *The reference epoch is given as a duration of time, in days, away from 1 Jan 2017 00:00:00 Ephemeris Time.

#	Δ Reference Epoch* (days)	τ (deg)	EL_1 / EL_2	C3 (km^2/s^2)	Transfer Δt (days)	# Earth Flybys	# Lunar Flybys	Injection Inclination (deg) Equatorial	Ecliptic
1	12.060302	334.519	2	−0.2902	133.76	0	0	23.225	28.192
2	12.211055	333.736	2	−0.3457	132.91	0	0	131.701	151.274
3	14.170854	283.655	2	−0.3444	118.36	0	0	51.319	69.045
4	15.226131	271.069	2	−0.4944	108.76	0	1	32.329	51.431
5	15.829146	279.419	2	−0.4296	171.62	0	0	85.326	103.860
6	20.351759	238.347	2	−0.6556	130.11	0	0	115.737	137.694
7	20.351759	239.232	2	−0.5856	145.20	0	0	21.877	22.738
8	22.311558	221.171	2	−0.6904	137.51	0	1	35.973	13.527
9	23.819095	206.901	2	−0.7153	129.17	0	0	22.180	10.275
10	20.050251	180.970	2	−1.8533	171.79	0	1	97.684	92.972
11	25.025126	164.113	2	−1.9222	146.35	0	1	20.490	4.271
12	27.286432	137.373	2	−2.0307	176.72	0	2	38.302	36.809
13	28.190955	168.405	2	−2.0880	122.46	2	2	19.325	30.359
14	28.040201	185.608	2	−1.0318	145.08	0	1	34.251	11.315
15	28.040201	185.630	2	−1.6144	145.75	0	2	103.995	126.244
16	0.000000	55.325	2	−0.9032	179.35	2	1	143.590	121.792
17	0.150754	63.382	2	−0.6429	97.90	0	0	23.372	0.836
18	0.452261	54.781	2	−0.6608	132.55	0	0	145.538	168.969
19	1.507538	66.990	2	−1.1266	113.39	0	1	166.454	144.152
20	8.592965	59.539	2	−0.8393	178.32	0	1	99.214	87.676
21	8.592965	59.962	2	−0.6791	165.37	0	0	14.732	20.434
22	6.030151	144.580	2	−0.6940	170.11	0	3	23.140	17.669
23	27.889447	53.118	2	−0.9637	140.22	1	2	11.452	28.632
24	28.040201	15.470	2	−0.4261	172.37	0	1	27.743	40.712
25	28.190955	34.787	2	−0.5891	105.30	0	0	148.336	171.495
26	28.341709	43.756	2	−0.5740	96.55	0	0	20.962	3.797
#	Δ Reference Epoch* (days)	τ (deg)	EL_1 / EL_2	C3 (km^2/s^2)	Transfer Δt (days)	# Earth Flybys	# Lunar Flybys	Injection Inclination (deg) Equatorial	Ecliptic
27	2.110553	245.420	1	−0.5465	91.66	0	0	20.003	4.747
28	2.412060	247.372	1	−0.6290	172.42	1	0	54.249	30.825
29	2.110553	251.704	1	−0.6311	178.46	1	2	59.547	36.213
30	2.261307	255.586	1	−0.5150	154.75	0	0	65.164	44.035
31	6.934673	122.568	1	−0.7340	165.38	0	0	20.624	28.138
32	6.783920	138.709	1	−0.5098	164.58	0	2	124.809	129.384
33	11.457286	38.141	1	−1.1299	167.55	0	2	39.917	26.275
34	14.170854	65.695	1	−0.5599	143.25	0	0	19.771	14.374
35	14.170854	70.107	1	−0.6869	123.22	0	0	106.493	129.791
36	14.170854	73.417	1	−0.6246	115.20	0	0	87.048	110.261
37	16.733668	222.850	1	−0.7658	179.64	0	1	137.534	126.323
38	16.733668	223.945	1	−0.6178	171.17	0	0	11.994	14.627
39	17.035176	192.365	1	−1.5154	156.53	1	1	28.596	51.902
40	22.160804	108.406	1	−2.0107	129.17	0	1	18.754	5.377
41	23.819095	87.587	1	−0.6915	167.13	0	0	50.748	32.372
42	28.190955	313.713	1	−0.4043	177.60	0	0	140.309	130.765
43	28.492462	285.732	1	−0.4568	109.17	0	1	10.097	14.214
44	3.165829	227.614	1	−1.9572	169.47	7	2	153.358	172.197

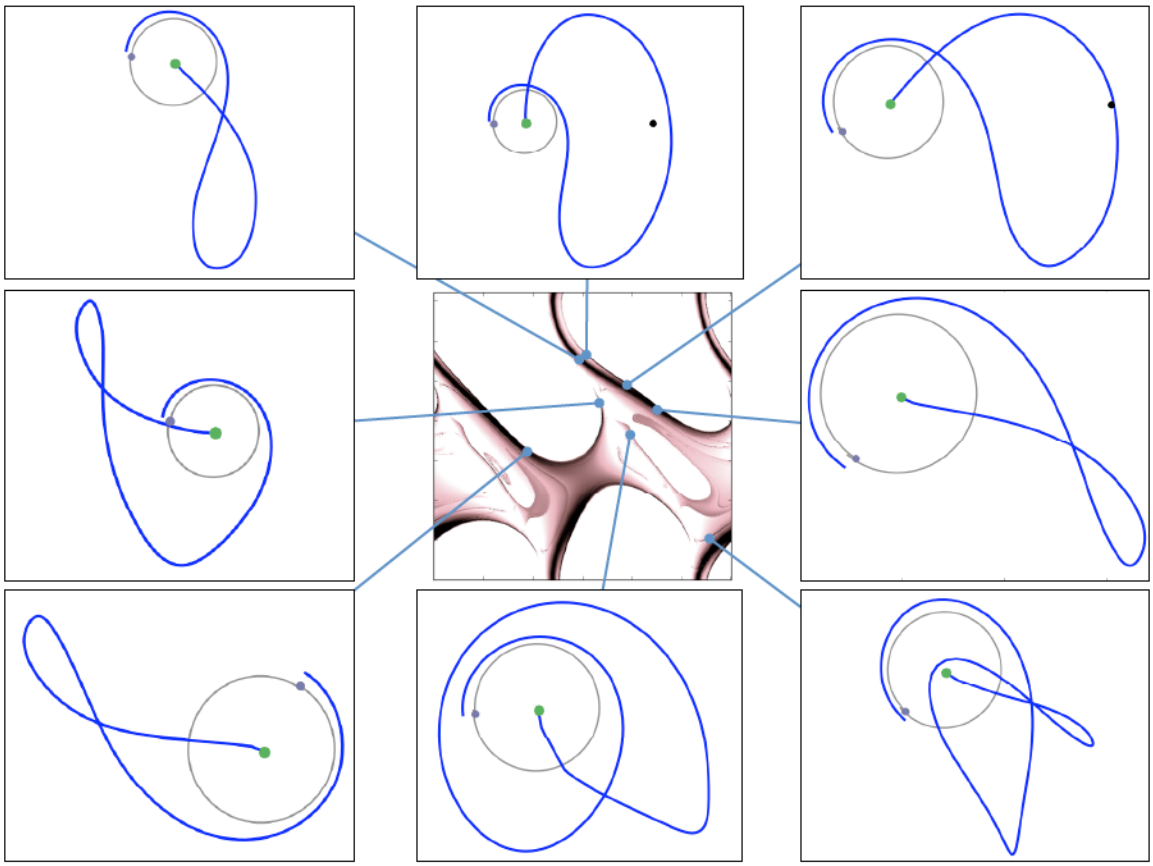

Figure 15 The same state space map shown in Figure 14 with example BLTs shown around the perimeter.

majority of the transfers shown require a launch energy in the range of -0.75 km^2/s^2 $\leq$ C3 ≤ -0.35 km^2/s^2. The transfers that include a lunar flyby often require less launch energy, particularly those that involve a lunar flyby on the outbound trajectory soon after injection. Several BLTs have been identified that require a C3 as low as -2.1 km^2/s^2, implementing a lunar flyby at an altitude of approximately 2000 km. Figure 17 shows the relationship between the required injection C3 and the transfer duration; Figure 18 compares the required injection C3 with the lowest lunar periapse altitude. One can see a clear correlation in Figure 18 that the closer a trajectory gets to the Moon during the transfer, the lower the injection C3 may be. Additional lunar flybys or Earth phasing orbits may help provide the geometry needed for a particular mission.

The BLT state space map shown in Figures 14 – 16 will repeat perfectly from one synodic month to the next in the Patched Three-Body Model, since the model is symmetric. The characteristics of the BLT state space map generated in the DE421 model of the solar system will vary from one synodic month to the next, although similar features will repeat. Figure 19 shows a map of the perigee altitude of trajectories generated from the same set of parameters presented in Table 2, but for a wider range of T_{ref} and τ: T_{ref} is varied over three months and τ is varied over two halo orbit revolutions. One can see the same features from cycle to cycle, but the details of the state space map vary. Significant variations are observed between the first halo orbit revolution ($0° \leq \tau \leq 360°$) and the second ($360° \leq \tau \leq 720°$), mostly as a consequence of the non-zero eccentricity of the

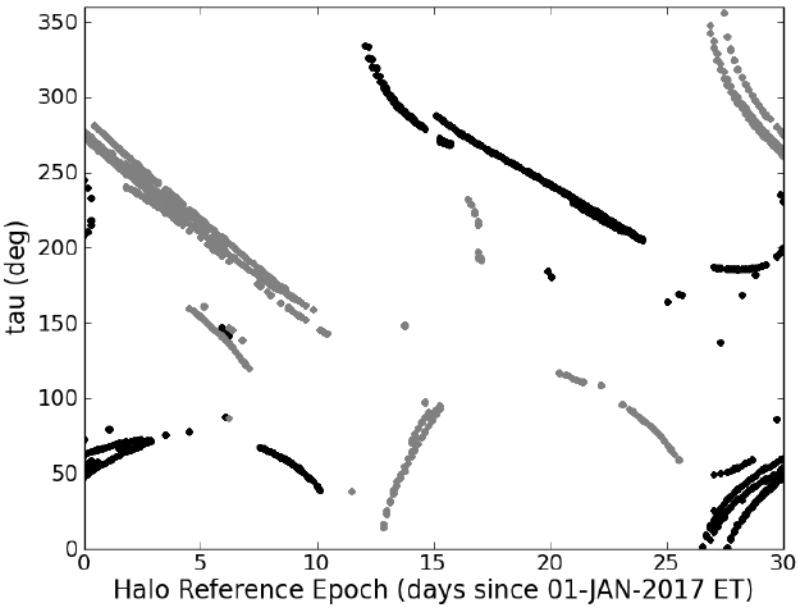

Figure 16 Combinations of T_{ref} and τ that generate BLTs with perigee injections at an altitude of 185 km. The points displayed in black correspond to trajectories that traverse closer to EL_2 than EL_1; points shown in gray travel closer to EL_1 than EL_2.

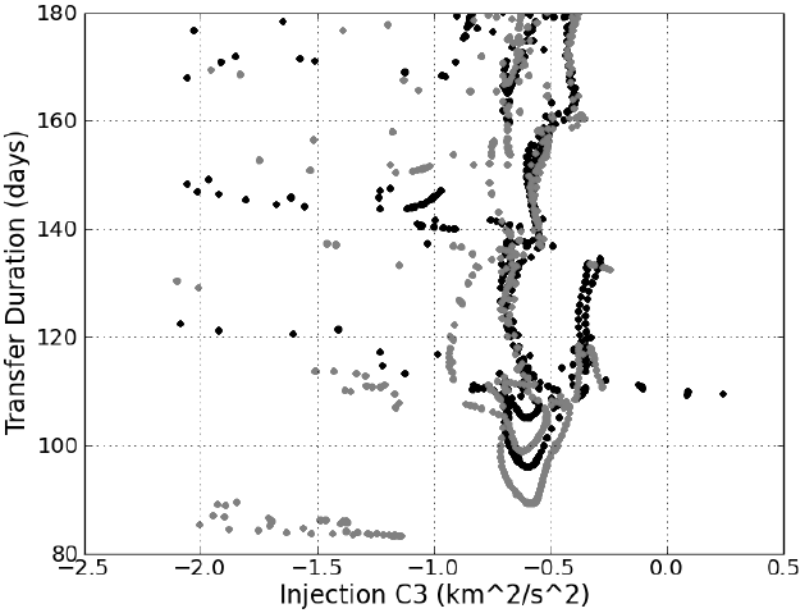

Figure 17 The relationship between the injection C3 value and the duration of the transfer for each BLT identified in Figure 16. The points displayed in black correspond to trajectories that traverse closer to EL_2 than EL_1.

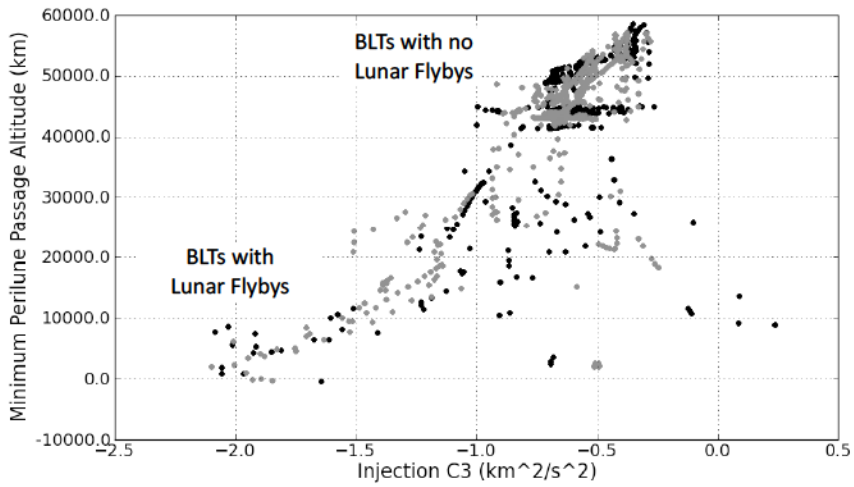

Figure 18 The relationship between the injection C3 value and the lowest lunar periapse altitude during each ballistic lunar transfer identified in Figure 16. The points displayed in black correspond to trajectories that travel closer to EL_2 than EL_1.

Moon's orbit about the Earth-Moon barycenter.

Ballistic lunar transfers between the Earth and a halo orbit with reference epochs that span the course of an entire year are compared in a single state space map by wrapping the transfers into a synodic month. Figure 20 compares the locations of BLTs in such a map, identifying the relationship between T_{ref} and τ across an entire year, where the abscissa axis of the plot displays the duration of time between T_{ref} and the beginning of the current synodic month, rather than T_{ref} directly.

The features observed in many performance characteristics of the identified BLTs repeat from synodic month to month. Figure 21 shows the relationship between the required injection C3 and the transfer duration for each identified BLT in a year, shaded according to the BLT's synodic month; Figure 22 compares the injection C3 with the minimum perilune altitude. One can see very discernable patterns in the BLT parameter relationships that repeat in each synodic month shown.

The largest variations observed from one synodic month to the next correspond to differences in the BLT injection inclination, in both equatorial and ecliptic reference frames, as illustrated in Figure 23. It is apparent when studying the plots shown in Figure 23 that BLTs depart the Earth from orbital planes at nearly any inclination during each synodic month. It is expected that the equatorial inclination of the BLT injection points will vary from one synodic month to the next due to the Earth's obliquity angle, however, significant variations also exist from month to month when observing the BLT injection points' ecliptic inclination values. The variations in the geometry during the year have a more pronounced effect when the trajectories fly near the Earth or Moon.

Discussion

The techniques described here to produce and analyze BLT state space maps may be extended to build state space maps of transfers between the Earth and any unstable three-body orbit in the Earth-Moon system. This paper has limited the scope of this exploration to a very specific type of transfer: one that is designed to transfer from 185 km above the Earth's surface to a specific LL_2 halo orbit via that orbit's exterior stable manifold using only the tangential injection maneuver and

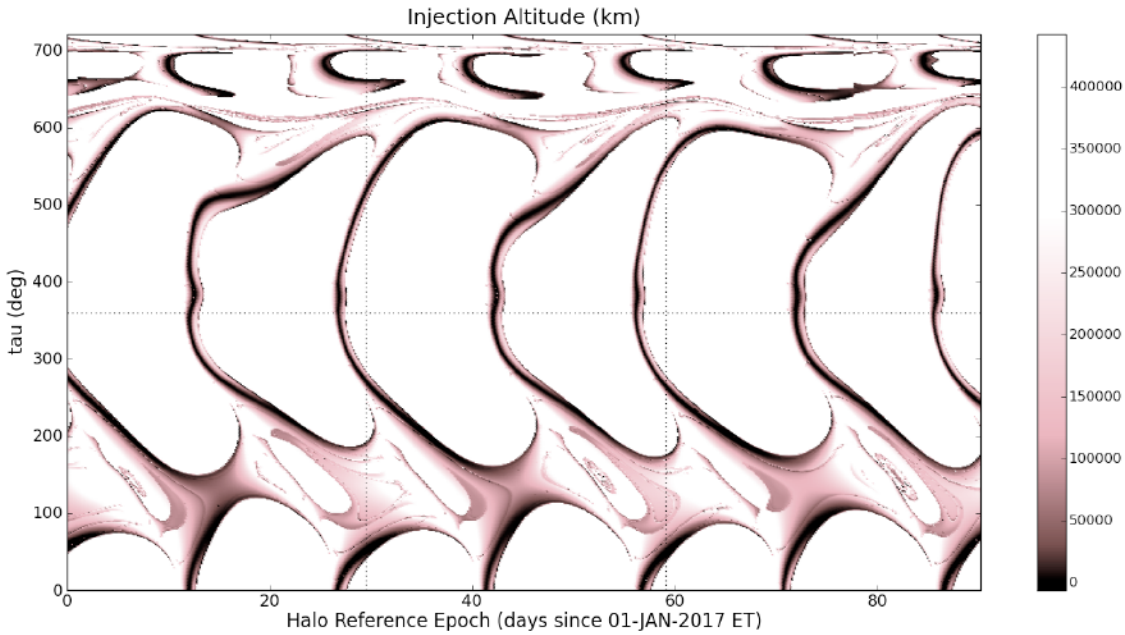

Figure 19 The same state space map shown in Figure 14 extended to cover 90 days of reference epochs and two revolutions of the halo orbit.

no more than 180 days of transfer time. Clearly the potential trade space of BLTs is very large. Nevertheless, even the limited scope of this paper identified a large number of families of BLTs, departing from the Earth each and every day at nearly any injection inclination.

The techniques presented here may be applied to the problem of transferring a spacecraft from any arbitrary orbit onto a trajectory to the Moon. It may be the case that a spacecraft is already in some orbit about the Earth and must then transfer onto a low-energy BLT – this has been the case with the two Artemis spacecraft.[1] In the case of Artemis, the two spacecraft were stationed in high orbits about the Earth prior to any consideration of how they would transfer onto a low-energy lunar transfer. A BLT state space map may be catered to these unique needs by tracing contours in the maps of BLT parameters that correspond to the specific mission requirements, e.g., contours of altitude and equatorial inclination that intersect the initial orbit.

It should be noted that the process of constructing a low-energy BLT in the DE421 model is not strictly smooth. The multiple shooting differential corrector iterates until a trajectory is generated that is continuous in position and velocity within some tolerance. In general, a very small change in an input parameter to the differential corrector, e.g., A_z, will yield a very similar trajectory. However, there are rare discontinuities between trajectories that are theoretically adjacent in a family of BLTs – discontinuities that result from a distinct change in the number of iterations required in the differential correction process. In addition, round-off error may present slight discontinuities in the characteristics of a family of BLTs due to the unstable nature of low-energy BLTs, their duration, and their potential interactions with the Earth and Moon. Finally, the parameters that produce a BLT on one machine using one integration scheme may not produce the exact same trajectory on another machine using different hardware and/or software due to the unstable nature of low-energy ballistic lunar transfers.

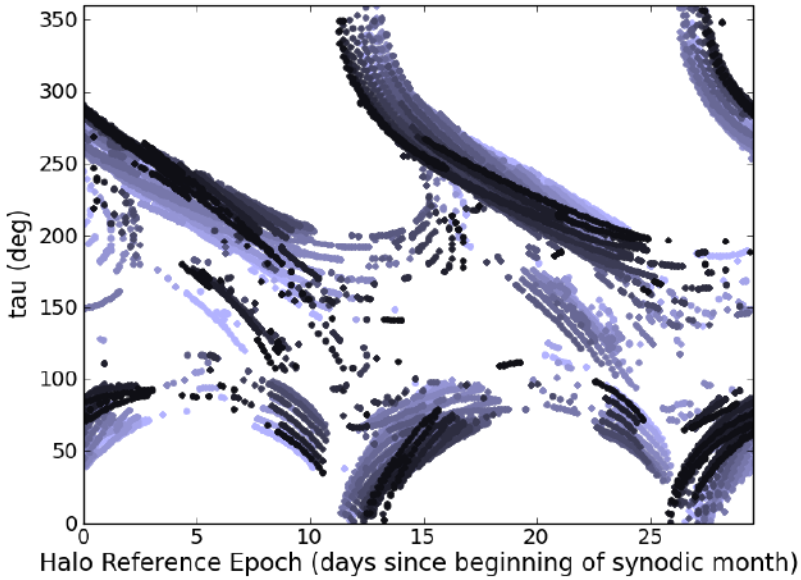

Figure 20 The combinations of T_{ref} and τ that yield BLTs during 12 months, relative to the beginning of each synodic month. The first month, which starts at a reference epoch of 1 Jan 2017 00:00:00 Ephemeris Time, is shown in the lightest shade and each consecutive synodic month thereafter is plotted in a darker shade.

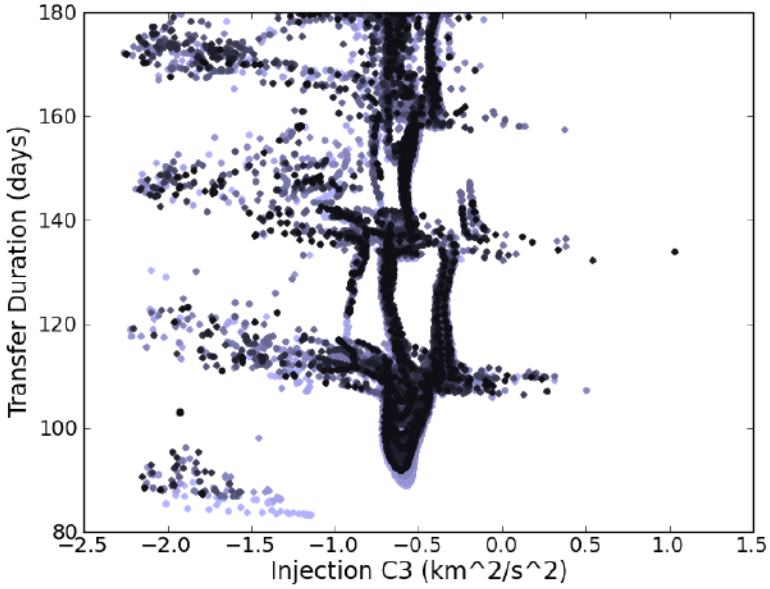

Figure 21 The relationship between the injection C3 value and the duration of the transfer for each BLT identified in Figure 20. The first month, which starts at a reference epoch of 1 Jan 2017 00:00:00 Ephemeris Time, is shown in the lightest shade and each consecutive synodic month thereafter is plotted in a darker shade.

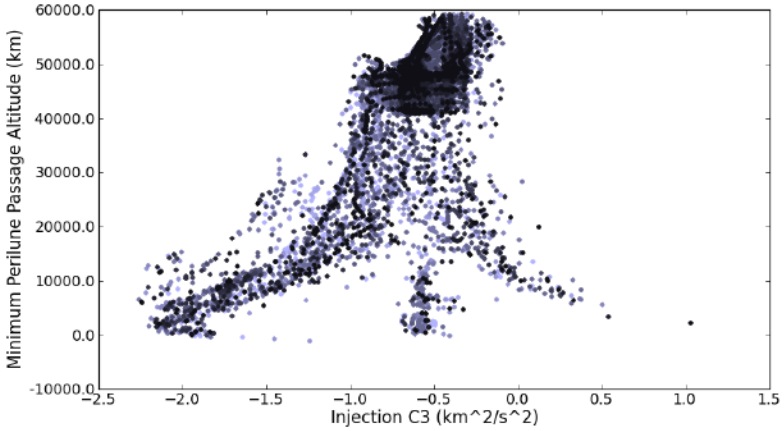

Figure 22 The relationship between the injection C3 value and the lowest lunar periapse altitude during each ballistic lunar transfer identified in Figure 20. The first month, which starts at a reference epoch of 1 Jan 2017 00:00:00 Ephemeris Time, is shown in the lightest shade and each consecutive synodic month thereafter is plotted in a darker shade.

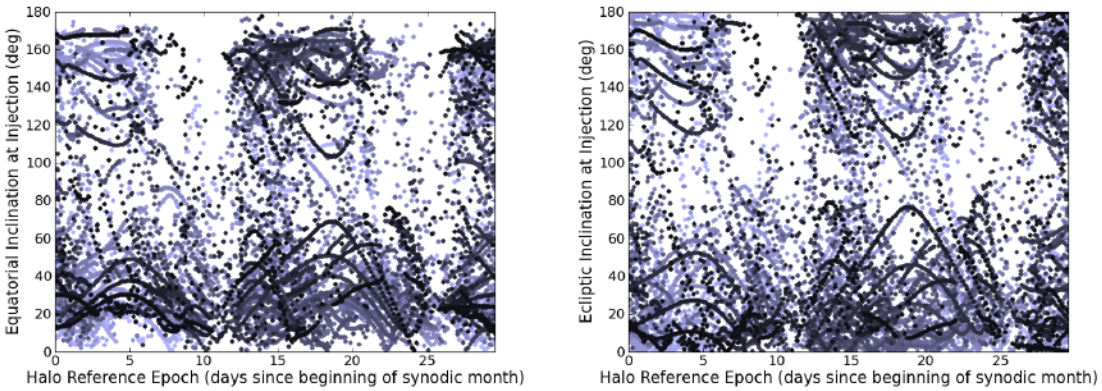

Figure 23 The equatorial (left) and ecliptic (right) inclination of the BLT injection point for each BLT identified in Figure 20. The first month, which starts at a reference epoch of 1 Jan 2017 00:00:00 Ephemeris Time, is shown in the lightest shade and each consecutive synodic month thereafter is plotted in a darker shade.

APPLICATIONS TO PRACTICAL MISSION DESIGN

Low-energy ballistic lunar transfers are a good trajectory choice for robotic missions to the Moon. They do not require any new technology; their transfer durations are operationally realistic; and they may be used to either reduce the fuel requirements of a mission or increase the payload mass of the system. A 100-day transfer is long enough to provide sufficient time for spacecraft check-out, trajectory correction maneuvers, and safety reviews prior to a critical event upon arrival at the Moon. Low-energy BLTs between the Earth and low lunar orbits or the surface of the Moon require less energy than conventional, direct trajectories. Missions to lunar three-body orbits, such as halo orbits, receive the greatest benefits by the implementation of a BLT. A BLT to an unstable halo orbit does not require a large orbit insertion maneuver – direct transfers, on the other hand, require

orbit insertions with ΔVs up to 500 m/s or more. Finally, low-energy ballistic transfers may also be constructed from lunar orbits to the Earth using the same theory. In those cases, low-energy transfers may be more flexible when targeting a specific entry condition upon arrival at the Earth.

CONCLUSIONS

Low-energy ballistic lunar transfers (BLTs) are constructed in this research using dynamical systems methods. Previous work has demonstrated how to build a BLT using dynamical systems theory in a simplified model of the solar system; this research extends that work into the more realistic DE421 model of the solar system, provided by the Jet Propulsion Laboratory at the California Institute of Technology.

This research has developed a method to build low-energy BLTs between the Earth and unstable three-body orbits at the Moon, such as halo orbits about either the Earth-Moon L_1 or L_2 point. It has been found that this technique provides a simple way to parameterize a BLT using only six parameters. These parameters may be systematically varied to identify and categorize families of BLTs. Given knowledge of these families of BLTs, a mission designer may be able to quickly survey a large variety of BLTs when selecting a trajectory for a specific mission.

Families of BLTs may be easily constructed and organized on a BLT state space map. It has been found that these state space maps vary from one synodic month to the next due to the asymmetric nature of the real solar system; yet many of the features do repeat from month to month. These features provide a means to quickly identify useful lunar transfers in a state space map in an arbitrary month.

ACKNOWLEDGMENT

The research described in this paper was carried out at the Jet Propulsion Laboratory, California Institute of Technology, under a contract with the National Aeronautics and Space Administration.

APPENDIX A: MULTIPLE SHOOTING DIFFERENTIAL CORRECTION

A multiple-shooting differential corrector is used in this paper to link many unstable trajectory segments together to form a single, fully continuous trajectory. This differential corrector may be characterized as an iterative algorithm, where each iteration involves two levels of differential correction. The algorithm is described in detail in the literature.[14,22,23]

The process begins by characterizing a trajectory by a set of segments, separated by patchpoints. Each trajectory segment is continuous in position and velocity, but the overall trajectory is not necessarily continuous across each patchpoint. The algorithm iteratively adjusts the state of each patchpoint in order to transform the set of trajectory segments into a single, continuous trajectory. The algorithm continues iterating until the resulting trajectory satisfies a set of desired constraints, e.g., continuity within some tolerance. The two levels of correction are described as follows.

Level I. The Level I differential correction process is a single-shooting algorithm that is designed to update the velocity of each patchpoint in the current sequence of segments, one at a time, such that the final state of each segment intersects the position and epoch of the following patchpoint. In this way, the Level 1 process transforms the set of discontinuous trajectory segments into a single trajectory that is continuous in position and time. The trajectory still includes velocity discontinuities at each patchpoint.

Level II. The Level II differential correction process updates the position and time of every patch-point in the trajectory simultaneously in order to reduce the sum of all velocity discontinuities in the trajectory. The result is a trajectory that is discontinuous in position, but has a reduction in total ΔV after the following execution of Level I.

Each pass through the two levels reduces the level of discontinuity in the trajectory, provided that the process is converging toward a continuous solution. Additional constraints may also be placed on the trajectory such that the process converges on a trajectory that meets specific mission design goals.[23]

REFERENCES

[1] S. B. Broschart, M. J. Chung, S. J. Hatch, J. H. Ma, T. H. Sweetser, S. S. Weinstein-Weiss, and V. Angelopoulos, "Preliminary Trajectory Design for the Artemis Lunar Mission," *AAS/AIAA Astrodynamics Specialist Conference*, No. AAS 09-382, Pittsburgh, Pennsylvania, AAS/AIAA, August 9–13, 2009.

[2] P. Xaypraseuth, "Gravity Recovery and Interior Laboratory (GRAIL) Project: Mission Plan," Tech. Rep. JPL D-38928, Jet Propulsion Laboratory, California Institute of Technology, 4800 Oak Grove Dr., Pasadena, CA 91109, November 2008.

[3] J. S. Parker, *Low-Energy Ballistic Lunar Transfers*. PhD thesis, University of Colorado, Boulder, Colorado, 2007.

[4] W. S. Koon, M. W. Lo, J. E. Marsden, and S. D. Ross, "Shoot the Moon," *AAS/AIAA Spaceflight Mechanics 2000*, Vol. 105, part 2, AAS/AIAA, 2000, pp. 1017–1030.

[5] W. S. Koon, M. W. Lo, J. E. Marsden, and S. D. Ross, "Low Energy Transfers to the Moon," *Celestial Mechanics and Dynamical Astronomy*, Vol. 81, September 2001, pp. 63–73.

[6] J. S. Parker and M. W. Lo, "Shoot the Moon 3D," *AAS/AIAA Astrodynamics Specialist Conference*, No. AAS 05-383, Lake Tahoe, CA, AAS/AIAA, August 7–11, 2005.

[7] J. S. Parker, "Families of Low-Energy Lunar Halo Transfers," *AAS/AIAA Spaceflight Dynamics Conference*, No. AAS 06-132, Tampa, FL, AAS/AIAA, January 22–26, 2006.

[8] J. S. Parker and G. H. Born, "Modeling a Low-Energy Ballistic Lunar Transfer Using Dynamical Systems Theory," *Journal of Spacecraft and Rockets*, Vol. 45, No. 6, 2008, pp. 1269–1281.

[9] V. Szebehely, *Theory of Orbits: The Restricted Problem of Three Bodies*. New York: Academic Press, 1967.

[10] W. M. Folkner, J. G. Williams, and D. H. Boggs, "The Planetary and Lunar Ephemeris DE 421," Tech. Rep. IOM 343R–08–003, Jet Propulsion Laboratory, California Institute of Technology, March 2008.

[11] R. W. Farquhar, *The Control and Use of Libration-Point Satellites*. PhD thesis, Department of Aeronautics and Astronautics, Stanford University, Stanford, CA, 1968.

[12] R. W. Farquhar, "Station-Keeping in the Vicinity of Collinear Libration Points with an Application to a Lunar Communications Problem," *Space Flight Mechanics*, Vol. 11 of *Science and Technology Series*, pp. 519–535, New York: American Astronautical Society, 1966.

[13] J. V. Breakwell and J. V. Brown, "The Halo Family of 3-Dimensional Periodic Orbits in the Earth-Moon Restricted 3-Body Problem," *Celestial Mechanics*, Vol. 20, November 1979, pp. 389–404.

[14] K. C. Howell, "Three-Dimensional, Periodic, 'Halo' Orbits," *Celes. Mech.*, Vol. 32, No. 1, 1984, pp. 53–71.

[15] A. C. Clarke, *Interplanetary Flight*. London: Temple Press Books Ltd., 1950.

[16] R. W. Farquhar, "Lunar Communications with Libration-Point Satellites," *Journal of Spacecraft and Rockets*, Vol. 4, No. 10, 1967, pp. 1383–1384.

[17] J. S. Parker and G. H. Born, "Direct Lunar Halo Orbit Transfers," *AAS/AIAA Spaceflight Mechanics Conference*, No. AAS 07-229, Sedona, Arizona, AAS/AIAA, January 28 – February 1, 2007.

[18] K. Hill, J. S. Parker, G. H. Born, and N. Demandante, "A Lunar L2 Navigation, Communication, and Gravity Mission," *AIAA/AAS Astrodynamics Specialist Conference*, No. AIAA 2006-6662, Keystone, Colorado, AIAA/AAS, August 2006.

[19] M. Hénon, "Numerical Exploration of the Restricted Problem. V., Hill's Case: Periodic Orbits and Their Stability," *Astronomy & Astrophysics*, Vol. 1, 1969, pp. 223–238.

[20] F. R. Moulton, "Periodic Orbits," *Carnegie Institute of Washington Publications*, No. 161, 1920.

[21] D. L. Richardson, "Analytical Construction of Periodic Orbits about the Collinear Points," *Celestial Mechanics*, Vol. 22, 1980, pp. 241–253.

[22] K. C. Howell and H. J. Pernicka, "Numerical Determination of Lissajous Trajectories in the Restricted Three-Body Problem," *Celes. Mech.*, Vol. 41, 1988, pp. 107–124.

[23] R. Wilson, "Derivation of Differential Correctors Used in GENESIS Mission Design," Tech. Rep. JPL IOM 312.I-03-002, Jet Propulsion Laboratory, California Institute of Technology, 2003.

[24] S. H. Strogatz, *Nonlinear Dynamics and Chaos*. Perseus Books Publishing, L.L.C., 1994.

[25] D. P. Muhonen, "Accelerometer-Enhanced Orbit Control Near the Sun-Earth L_1 Libration Point," *AIAA 21st Aerospace Sciences Meeting*, No. AIAA-83-0018, Reno, Nevada, AIAA, January 10–13, 1983.

[26] Limon, M., et al., "Wilkinson Microwave Anisotropy Probe (WMAP): Explanatory Supplement," Tech. Rep. 1.0, Goddard Space Flight Center, Greenbelt, MD: NASA/GSFC, February 11, 2003.

[27] N. G. Smith, K. E. Williams, R. C. Wiens, and C. E. Rasbach, "Genesis – The Middle Years," *IEEE Aerospace Conference*, Vol. 1, Big Sky, Montana, IEEE, 2003.

[28] K. E. Williams, G. D. Lewis, R. S. Wilson, C. E. Helfrich, and C. L. Potts, "Genesis Earth Return: Refined Strategies and Flight Experience," *AAS/AIAA Space Flight Mechanics Conference*, No. AAS 05-116, Copper Mountain, CO, AAS/AIAA, January 23–27, 2005.

[29] G. Gómez, W. S. Koon, M. W. Lo, J. E. Marsden, J. Masdemont, and S. D. Ross, "Invariant Manifolds, the Spatial Three-Body Problem and Space Mission Design," *AIAA/AAS Astrodynamics Specialist Meeting*, No. AIAA 01-301, Quebec City, Canada, AIAA/AAS, August 2001.

[30] S. Wiggins, *Introduction to Applied Nonlinear Dynamical Systems and Chaos*. Text in Applied Mathematics, 2, New York: Springer-Verlag, 1990.

[31] G. Gómez, W. S. Koon, J. E. Marsden, J. Masdemont, and S. D. Ross, "Connecting Orbits and Invariant Manifolds in the Spatial Restricted Three-Body Problem," *Nonlinearity*, Vol. 17, September 2004, pp. 1571–1606.

[32] S. D. Ross, *Cylindrical Manifolds and Tube Dynamics in the Restricted Three-Body Problem*. PhD thesis, California Institute of Technology, April 2004.

[33] G. Gómez, A. Jorba, A. Masdemont, and C. Simó, "Study of the Transfer Between Halo Orbits," *Acta Astronautica*, Vol. 43, November 1998, pp. 493–520.

[34] C. Conley, "Low Energy Transit Orbits in the Restricted Three Body Problem," *SIAM Journal Appl. Math.*, Vol. 16, No. 4, 1968, pp. 732–746.

[35] E. A. Belbruno, "Lunar Capture Orbits, a Method of Constructing Earth Moon Trajectories and the Lunar Gas Mission," *The 19th AIAA/DGLR/JSASS International Electric Propulsion Conference*, No. AIAA 87-1054, Colorado Springs, Colorado, May 1987.

[36] E. A. Belbruno and J. P. Carrico, "Calculation of Weak Stability Boundary Ballistic Lunar Transfer Trajectories," *AIAA/AAS Astrodynamics Specialist Conference*, No. AIAA 2000-4142, Denver, CO, AIAA/AAS, 14-17 August 2000.

[37] E. A. Belbruno, *Capture Dynamics and Chaotic Motions in Celestial Mechanics*. Princeton University Press, Princeton, NJ, 2004.

[38] H. Yamakawa, J. Kawaguchi, N. Ishii, and H. Matsuo, "On Earth-Moon Transfer Trajectory with Gravitational Capture," *AIAA/AAS Astrodynamics Specialist Conference*, No. AIAA 93-633, AIAA/AAS, August 1993.

[39] V. V. Ivashkin, "On Trajectories of the Earth-Moon Flight of a Particle with its Temporary Capture by the Moon," *Doklady Physics, Mechanics*, Vol. 47, No. 11, 2002, pp. 825–827.

[40] V. V. Ivashkin, "On the Earth-to-Moon Trajectories with Temporary Capture of a Particle by the Moon," *54th International Astronautical Congress*, No. Paper IAC-03-A.P.01, Bremen, Germany, Sept. 29–Oct. 3, 2003, pp. 1–9.

[41] V. V. Ivashkin, "On Trajectories for the Earth-to-Moon Flight with Capture by the Moon," *International Lunar Conference 2003* (Steve M. Durst, et al., ed.), Vol. 108 of *Science and Technology Series*, American Astronautical Society AAS, 2004, pp. 157–166.

[42] V. V. Ivashkin, "On Particle's Trajectories of Moon-to-Earth Space Flights with the Gravitational Escape from the Lunar Attraction," *Doklady Physics, Mechanics*, Vol. 49, No. 9, 2004, pp. 539–542.

[43] C. G. Schroer and E. Ott, "Targeting in Hamiltonian Systems that have Mixed Regular/Chaotic Phase Spaces," *Chaos*, Vol. 7, December 1997, pp. 512–519.

[44] E. M. Bollt and J. D. Meiss, "Targeting Chaotic Orbits to the Moon Through Recurrence," *Physics Letters A*, Vol. 204, pp. 373–378, August 1995.